

JOINT VERTICAL SHEAR RESISTANCE OF STEEL PIPE SHEET PILE CONSIDERING CONFINING PRESSURE

Kyoto University Student Member ○Junxiong Peng

Kyoto University Regular Member Yuusuke Miyazaki, Yasuo Sawamura

Hanshin Expressway Co., Ltd. Regular Member Takashi Kosaka, Tomohiko Nishihara,
Masatsugu Shinohara

Hanshin Expressway Research Institute for Advanced Technology Regular Member Masahiro Hattori

1. OVERVIEW

The steel pipe sheet pile (SPSP) foundation has been widely constructed as a unique structure satisfying both the roles of the waterproof wall and the supporting foundation of superstructures. The series of FEM analyses on SPSP models under lateral loading by Miyazaki et al. (2021) clarified that the vertical shear forces of the joint part exceed compressive and tensile forces. (Fig. 1). Besides, Inazumi et al. (2009) found that the vertical shear resistance of the joint without confining pressure could be extrapolated based on the direct shear test on a steel-mortar plate. Therefore, the stress-dependency of the joint vertical shear resistance can be one of the issues to be clarified. Our research group designed an SPSPs model, the joint part of which has quasi-brittle mechanical behaviors similar to the actual SPSP foundation. Through the vertical shear test on the joint part under different confining pressures, we tried to clarify the effect of the confining pressure on the vertical shear behaviors of the joint part.

2. OUTLINE OF EXPERIMENT

The SPSPs model is shown in Fig. 2. The past report can refer to the joint model's compressive, tensile strength, and failure modes (Peng et al., 2021). Fig. 3 shows the schematic drawing of the vertical shear test. An MTS unconfined compressive servo system (661,238-01 for the vertical load) was used to apply the vertical shear load on the middle block jig. An air cylinder (FUJIKURA BF CYLINDER, FCD-31.5-35) was used to offer the constant confining pressure to the side of the block jig. The lateral deformation of the joint part was measured using a contacting displacement meter. Ball rollers were installed to the side and bottom of the block jig to eliminate the friction between the models and the rectangular-shaped jig. The loading velocity is 1 mm/min, the same as the previous vertical shear test (Kusaba et al., 2018). The applied confining pressure considered the earth pressure at the different depths from the ground surface. The length of the SPSPs model planned to be used in the following centrifuge load test is 25.5m, and the earth pressures at the depths of 0.13 m, 12.25 m, and 25.5 m were considered. The confining load applied by the air cylinder was converted from the equation below:

$$F = A\sigma = A\gamma h k = A\gamma h \tan^2(45^\circ - \Phi/2) \quad (1)$$

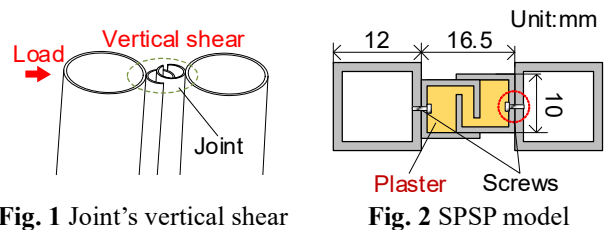


Fig. 1 Joint's vertical shear

Fig. 2 SPSP model

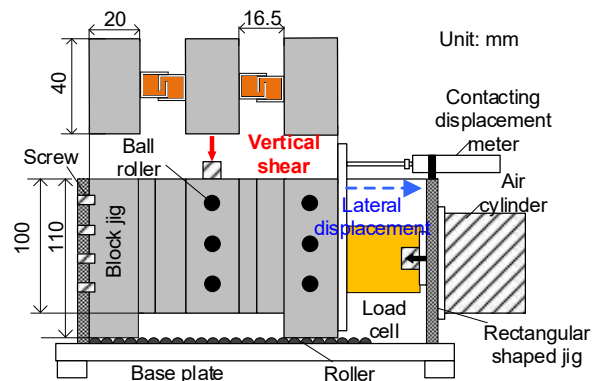


Fig. 3 Schematic drawing of the vertical shear test

Where, F is the confining load applied to the side of the block jig (N), A is the area of the side of the block jig (0.001 m^2), γ is the unit volume weight of the ground made by Toyoura sand, which is the material of the ground model in the centrifuge load test (25.48 N/m^3), h is the depth (m), Φ is the friction angle of Toyoura sand (38.73°). The relative density of Toyoura sand was set to be 90%. The load was calculated as 0.02 kN, 0.1 kN, and 0.2 kN. Three tests were conducted for each confining load in the vertical shear tests.

3. RESULTS OF THE VERTICAL SHEAR TEST

Fig. 4 shows the result of the vertical shear test. The horizontal axis is the normalized axial displacement (L_V/D): vertical shear displacement, L_V , divided by the pipe diameter, $D = 15 \text{ mm}$. The vertical axis is defined by the stress ratio, τ/σ , which is calculated as follows:

$$\tau/\sigma = (F_V/A) / (F_N/A) \quad (2)$$

Where τ/σ is the stress ratio by the vertical shear stress, τ , and the confining stress, σ , F_V is the measured vertical shear force from the load cell [kN], A is the vertical cross-sectional area of the joint [mm^2] ($A = 1000 \text{ mm}^2$), and F_N is the confining force [kN] applied by the air cylinder. τ/σ reflects the vertical shear resistance of the

Keywords: SPSP foundation, joint, vertical shearing, confining pressure

Contact address: Katsura Campus, Kyoto University, Nishikyo-ku, Kyoto, 615-8540, Japan, Tel: +81-(75-383-3231)

joint depending on the confining pressure. In the cases of the confining load of 0.02 and 0.1 kN, the lateral displacement of the model (L_H) was measured, and the normalized lateral displacement (L_H/D) was shown, respectively.

Take the test of confining 0.1 kN as an example. According to **Fig. 4**, the stress ratio reached the first yielding in the L_V/D at around 0.01 and kept relatively steady until 0.03. The stress ratio reached the peak value at the L_V/D of 4.5%, and **Fig. 5** exhibits the model of this time. The vertical slide separation between the gypsum plaster and the inner metal part of the joint occurred. The curve tended to be stable after the peak.

From the figures, the stress ratio increased intensively within the L_V/D of 0 ~ 0.05. L_H/D has also mainly changed in the same range. The yielding points of the L_H/D have the closing L_V/D to the yielding points of the stress ratio, which means the joint's dilatancy (volume variation) phenomenon occurs with the vertical shear process. Besides, when the stress ratio tended to be stable after the L_V/D of 0.05, the L_H/D also remained stable.

Fig. 6 shows the peak vertical shear strength of the joint under different confining loads. The peak shear strength increases from 0.25 to 4.20 kN/m when the confining load is set from 0.1 to 0.2 kN. However, the peak shear strength changed little when the confining load was set from 0.02 to 0.1 kN. This study considered there might be a threshold value of confining load for the confining stress-dependency of the vertical shear behavior. When the confining pressure is smaller than a particular value, the effect on the vertical shear strength of the joint will be unclear. Within a certain range, the confining pressure enlarges the vertical shear force.

4. CONCLUSION

Focusing on the vertical shear behaviors of the joints of the SPSP foundation, this study designed an SPSP foundation model whose joint part has similar quasi-brittle behaviors as the actual SPSP foundation. Through the vertical shear test on the joint model with different confining pressures, this paper clarified the vertical shear behaviors of the joint model with the consideration of the confining pressure-dependency. The failure mode (behaviors of the specimen when yields) was found as the vertical sliding separation between the filling material and the inner metal part of the joint. Besides, the dilatancy phenomenon during the shear process was found by measuring the joint's lateral displacement. On the other hand, this study found there might be a threshold value of the confining pressure in terms of the effects on the shear behaviors. The confining stress-dependency will occur if it exceeds a certain range.

ACKNOWLEDGEMENT

The third author was supported by the JSPS KAKENHI, Grant No.19K15087.

REFERENCES

- Miyazaki, et al. (2021): Numerical analysis on mechanical characteristics of joint structure of a steel pipe sheet pile foundation. Proc. of the 16th IACMAG. pp. 59-67.
- Inazumi, et al. (2009): Evaluation of Mechanical Characteristics of Joint Sections in Steel Pipe Sheet Piles and Development of 3D-Frame Structural analysis on Design of SPSP Foundations. Journal of JSCE C. Vol. 65. No. 2. 532-543. (In Japanese)
- Peng, et al. (2021): Mechanical tests on joint part using plaster as filling material for steel pipe sheet pile model, the 56th annual conference of JGS, No. 13-8-5-04.
- Kusaba, et al. (2019): Mechanical test on joint part of steel pipe sheet pile foundation modeling shape of joint and lateral loading test on one element of SPSP foundation, the 54th annual conference of JGS, pp.1173-1174. (in Japanese)

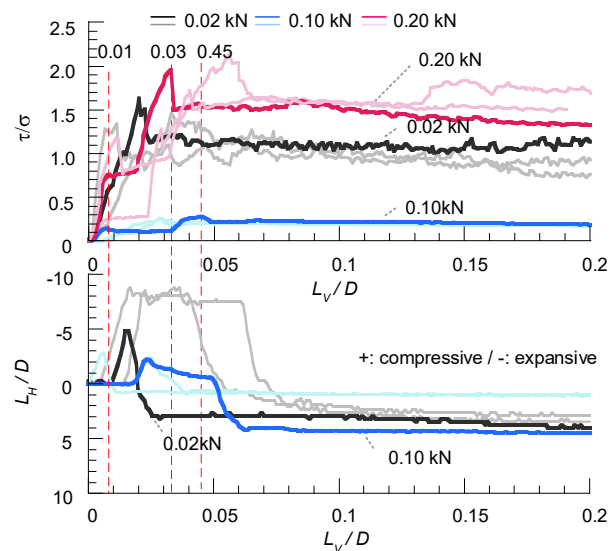


Fig. 4 $\tau/\sigma, L_H/D$ – Normalized axial displacement curve

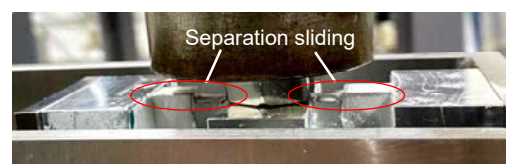


Fig. 5 The model when yields

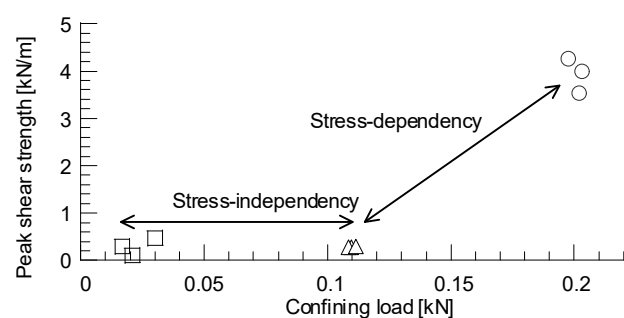


Fig. 6 Peak shear resistance values